



UvA-DARE (Digital Academic Repository)

Early Response to Dehydration 7 Remodels Cell Membrane Lipid Composition During Cold Stress in Arabidopsis

de Dios Barajas-Lopez, J.; Tiwari, A.; Zarza, X.; Shaw, M.W.; Pascual, J.; Punkkinen, M.; Bakowska, J.C.; Munnik, T.; Fujii, H.

DOI

[10.1093/pcp/pcaa139](https://doi.org/10.1093/pcp/pcaa139)

Publication date

2021

Document Version

Final published version

Published in

Plant and Cell Physiology

License

Article 25fa Dutch Copyright Act

[Link to publication](#)

Citation for published version (APA):

de Dios Barajas-Lopez, J., Tiwari, A., Zarza, X., Shaw, M. W., Pascual, J., Punkkinen, M., Bakowska, J. C., Munnik, T., & Fujii, H. (2021). Early Response to Dehydration 7 Remodels Cell Membrane Lipid Composition During Cold Stress in Arabidopsis. *Plant and Cell Physiology*, 62(1), 80–91. <https://doi.org/10.1093/pcp/pcaa139>

General rights

It is not permitted to download or to forward/distribute the text or part of it without the consent of the author(s) and/or copyright holder(s), other than for strictly personal, individual use, unless the work is under an open content license (like Creative Commons).

Disclaimer/Complaints regulations

If you believe that digital publication of certain material infringes any of your rights or (privacy) interests, please let the Library know, stating your reasons. In case of a legitimate complaint, the Library will make the material inaccessible and/or remove it from the website. Please Ask the Library: <https://uba.uva.nl/en/contact>, or a letter to: Library of the University of Amsterdam, Secretariat, Singel 425, 1012 WP Amsterdam, The Netherlands. You will be contacted as soon as possible.

UvA-DARE is a service provided by the library of the University of Amsterdam (<https://dare.uva.nl>)

EARLY RESPONSE TO DEHYDRATION 7 Remodels Cell Membrane Lipid Composition during Cold Stress in Arabidopsis

Juan de Dios Barajas-Lopez¹, Arjun Tiwari¹, Xavier Zarza², Molly W. Shaw³, Jesús Pascual¹, Matleena Punkkinen¹, Joanna C. Bakowska⁴, Teun Munnik ², and Hiroaki Fujii ¹

¹Molecular Plant Biology Unit, Department of Biochemistry, University of Turku, Turku 20014, Finland

²Section Plant Cell Biology, Swammerdam Institute for Life Sciences (SILS), University of Amsterdam, Science Park 904, Amsterdam, XH 1098, Netherlands

³Department of Hematology, Cincinnati Children's Hospital Medical Center, Cincinnati, OH 45229, USA

⁴Department of Molecular Pharmacology and Therapeutics, Stritch School of Medicine, Loyola University Chicago, Maywood, IL 60153, USA

Corresponding author: E-mail, hiroaki.fujii@utu.fi; Fax, +358-29-450-5040.

(Received 22 April 2019; Accepted 24 October 2020)

Plants adjust to unfavorable conditions by altering physiological activities, such as gene expression. Although previous studies have identified multiple stress-induced genes, the function of many genes during the stress responses remains unclear. Expression of *ERD7* (*EARLY RESPONSE TO DEHYDRATION 7*) is induced in response to dehydration. Here, we show that *ERD7* plays essential roles in both plant stress responses and development. In *Arabidopsis*, *ERD7* protein accumulated under various stress conditions, including exposure to low temperature. A triple mutant of *Arabidopsis* lacking *ERD7* and two closely related homologs had an embryonic lethal phenotype, whereas a mutant lacking the two homologs and one *ERD7* allele had relatively round leaves, indicating that the *ERD7* gene family has essential roles in development. Moreover, the importance of the *ERD7* family in stress responses was evidenced by the susceptibility of the mutant lines to cold stress. *ERD7* protein was found to bind to several, but not all, negatively charged phospholipids and was associated with membranes. Lipid components and cold-induced reduction in PIP_2 in the mutant line were altered relative to wild type. Furthermore, membranes from the mutant line had reduced fluidity. Taken together, *ERD7* and its homologs are important for plant stress responses and development and associated with the modification in membrane lipid composition.

Keywords: Arabidopsis • Cold stress • ERD7 • Membrane lipid composition.

Introduction

Plants have developed several mechanisms to adapt in response to unfavorable growth conditions. Understanding the mechanisms involved in sensing stress signals and triggering adaptive mechanisms are fundamental biological questions to address to improve plant stress resistance. Cold stress is an environmental factor that has a significant impact on crop growth and limits the geographical distribution of many plants (Liu et al. 2019).

Low temperature can arrest plant growth and extended exposure to temperatures below 0°C disrupts cellular membranes, leading to cell death. However, most temperate plants can survive mild freezing after a period of exposure to low and non-lethal temperatures (between 12.5 and 4°C) in a process known as cold acclimation, which involves transcription and metabolic changes that increase the levels of intracellular solutes and metabolites. Cold acclimation also requires rapid and dynamic changes in lipid composition, since membrane stabilization is indispensable for survival in freezing conditions (Webb et al. 1994, Uemura et al. 1995, Zheng et al. 2011, Degenkolbe et al. 2012). During cold acclimation, the total amount of structural phospholipids, such as phosphatidylcholine (PC) and phosphatidylethanolamine (PE), increases in the plasma membrane (PM) (Degenkolbe et al. 2012). Galactolipids, including monogalactosyldiacylglycerol (MGDG) and digalactosyldiacylglycerol (DGDG), also play an important role during stress acclimation in plants. These two types of galactolipids are both primarily located in thylakoid membranes and chloroplast inner and outer envelope membranes. These lipids allow the insertion of the cold-regulated protein COR15A into thylakoid membranes during cold stress to stabilize the membranes and maintain the optimal efficiency of photosynthesis (Steponkus et al. 1998, Navarro-Retamal et al. 2018).

In addition, lipids can act as signal transducers to drive biological responses with phosphatidic acid (PA) and polyphosphoinositides (PPIs) being important mediators of stress signals (Munnik and Vermeer 2010, Munnik and Nielsen 2011, Heilmann 2016). PA can trigger a rapid biological response that occurs within seconds–minutes of exposure to a broad variety of stresses, including salinity, cold, drought, heat, wounding and pathogen attack (Arisz et al. 2013, Arisz et al. 2018, Tan et al. 2018). Several PA-binding proteins are directly involved in distinct biotic/abiotic stress-regulating plant responses (Testerink and Munnik 2011, Hou et al. 2016, Yao and Xue 2018). For example, PA-activated MPK6 phosphorylates Na^+/H^+ antiporter SOS1 under salt stress (Yu et al. 2010). Subcellular

localization of osmotic stress-activated kinase SnRK2.4 and 2.10 is mediated by PA (McLoughlin et al. 2012). Some intrinsically disordered proteins (Late Embryogenesis Abundant-like and Dehydrins) bind PA and enzymes and protect enzymes from damage by stresses (Eriksson et al. 2011, Petersen et al. 2012). Abscisic acid (ABA) responses are also mediated by several PA-binding proteins, such as ABI1 and RGS1 (Zhang et al. 2004, Roy Choudhury and Pandey 2017). Meanwhile PPIs are derived from phosphatidylinositol (PI) after phosphorylation of the lipid head group (Munnik and Vermeer 2010). PPIs are differentially distributed among the different cellular membranes and contribute to membrane trafficking events (Munnik and Nielsen 2011, Daboussi et al. 2012, Vermeer and Munnik 2013, Heilmann 2016, Noack and Jaillais 2017). Despite the importance of lipid in stress responses, knowledge about proteins mediating and regulating lipid plasticity during stress acclimation remains limited. The discovery of proteins that mediate or regulate lipid metabolism will serve to clarify the role of lipids during stress acclimation, being this of significant value for plant biotechnology applications.

Although gene expression of *ERD7* (EARLY RESPONSE TO DEHYDRATION 7) has been known to be related to drought stress for around 25 years (Kiyosue et al. 1994) and more recently it was linked to other stress conditions, such as cold, salt, excess light and Pi starvation (Kreps et al. 2002, Hammond et al. 2003, Kimura et al. 2003, Sánchez et al. 2004), the importance of *ERD7* remains obscure. *ERD7* contains a Senescence domain (Pfam: PF06911) that has lipid-binding activity (Joshi and Bakowska 2011). In this study, we examined the relationship between *ERD7* and lipid composition of cell membranes, as well as the effects that lipid alterations have on the fluidity of cellular membranes in Arabidopsis exposed to cold temperatures.

Results

ERD7 protein accumulates under low temperature

ERD7 mRNA expression is induced by abiotic stresses (Kiyosue et al. 1994, Taji et al. 1999). Here, we evaluated the amount of *ERD7* under abiotic stress with an anti-*ERD7* antibody produced using a specific *ERD7* peptide as an antigen to probe extracts from wild-type Arabidopsis plants and plants having a T-DNA insertion in *ERD7*. In extracts from plants exposed to low temperature (4°C, 24 h), Western blotting detected a 58-kDa band in wild type but not the *erd7* mutant, indicating that *ERD7* protein accumulates in response to cold (Fig. 1, Supplementary Fig. S1A). NaCl and ABA treatments also induced *ERD7* protein accumulation, but to a lesser extent than that seen for cold treatment (Fig. 1). These results indicated that *ERD7* also accumulated at the protein level in response to abiotic stresses. In subsequent experiments, we focused on the role of *ERD7* in response to cold stress conditions.

ERD7 binds to phospholipids in vitro

ERD7 has 452 amino acids and the C-terminal domain (aas 258–427) carries a plant Senescence domain, which is homologous

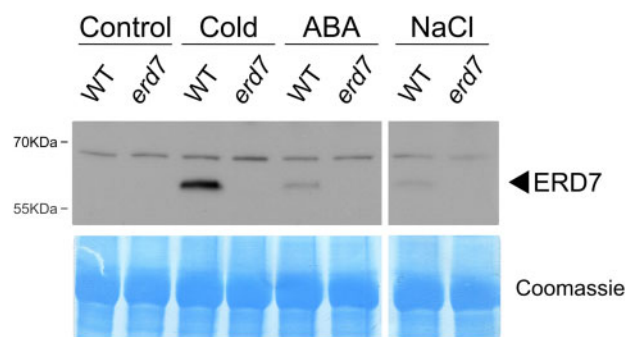


Fig. 1 *ERD7* protein accumulation in response to abiotic stress conditions. Western blot of total protein extracts from 10-day-old seedlings exposed to low temperature (4°C) for 24 h, 100 μM ABA or 100 mM NaCl for 1 h and probed with *ERD7* antibody.

(27% identity and 45% similarity in the BLAST analysis) to that in the human SPARTIN20 (SPG20) protein that mediates interactions between SPG20 and cardiolipin (Joshi and Bakowska 2011). Based on the high sequence similarity between Senescence domains of SPG20 and *ERD7*, we examined whether *ERD7* had lipid-binding activity. To test this, we expressed and purified a fusion protein consisting of a maltose-binding protein (MBP) fused to an *ERD7* peptide (aas 69–440) containing the Senescence domain (MBP-*ERD7*) from *Escherichia coli* (Fig. 2A, Supplementary Fig. S1B). The recombinant MBP-*ERD7* protein was used for an in vitro protein–lipid overlay assay using nitrocellulose membranes pre-spotted with phospholipids. As shown in Fig. 2B, MBP-*ERD7* interacted with cardiolipin, PA and all species of PPIs tested. These data indicated that *ERD7* interacts with several types of negatively charged phospholipids.

Arabidopsis has two closely related homologs of *ERD7*: AT3g51250 (hereafter *ERD7-like1*: *EDN1*) and AT4g35985 (hereafter *ERD7-like2*: *EDN2*), which have a pairwise identity of >62% based on the Clustal Omega analysis (EMBL-EBI). According to the GENEVESTIGATOR database (Hruz et al. 2008), the *ERD7* gene is highly responsive to abiotic stress conditions, such as drought, cold, osmotic and salt stress (Supplementary Fig. S2), whereas only cold and drought conditions triggered the upregulation of *EDN2* gene expression. Meanwhile, *EDN1* gene expression is not affected by any environmental stress (Supplementary Fig. S2). We cloned both *EDN1* and *EDN2* for further analysis. GST-fused forms of full-length *ERD7* and *EDN1* were produced in *E. coli* (Supplementary Fig. S1B). Unfortunately, GST-full-length *EDN2* could not be purified in our *E. coli* expression system. The TAIR database indicates that *EDN2* has splice variants and our RT-PCR amplified a splice variant of *EDN2*, in which the third intron was not spliced out, resulting in coding short form (M1-K384) of *EDN2* (*EDN2-S*, Supplementary Fig. S1C), in addition to the full-length *EDN2*. We successfully purified the *EDN2-S* protein from *E. coli* (Supplementary Fig. S1B). The anti-*ERD7* antibody used above did not recognize GST-*EDN1* or GST-*EDN2-S* (Supplementary Fig. S1D), suggesting no cross-reactivity to *EDN1* and *EDN2*.

A liposome flotation assay was performed to exclude the possibility that lipid association is due to the hydrophobicity of

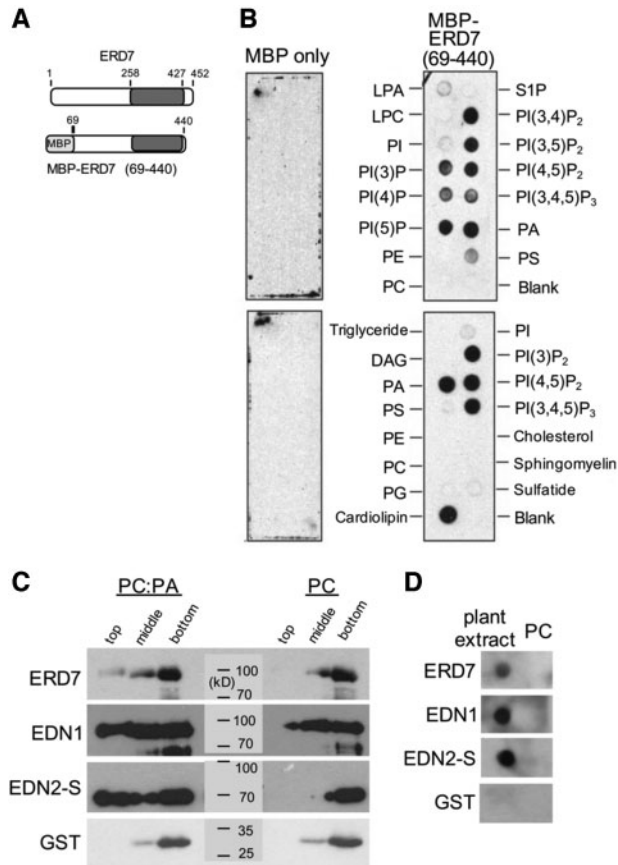


Fig. 2 The ERD7 Senescence domain binds to several phospholipid species. (A) Schematic diagram of ERD7 showing the MBP tag and the senescence domain enclosed by a gray box (258–427). (B) Lipid overlay assay with MBP-ERD7 or MBP alone. (C) Liposome flotation assay with GST-ERD7, GST-EDN1, GST-EDN2-S or GST. PC:PA (9:1) or PC only liposome was floated in the sucrose gradient. Top (containing liposome), middle and bottom fractions were loaded for Western blotting with an anti-GST antibody. (D) Lipid overlay assay with plant extract or egg yolk PC.

the ERD7 and to confirm the binding between ERD7 family and PA under further physiological conditions. GST-ERD7, GST-EDN1 and GST-EDN2-S, but not GST, were detected in the top fraction containing PC:PA (9:1) liposome, but not in the fraction containing PC-only liposome (Fig. 2C). These results suggest that ERD7 and homologs can bind to the PA head group. Furthermore, lipids extracted from Arabidopsis leaves were blotted for overlay assay to confirm the binding to plant lipids as well as commercially available lipids usually extracted from animals. GST-ERD7, GST-EDN1 and GST-EDN2-S, but not GST, bound to plant extract (Fig. 2D). These data suggest that ERD7 and two homologs bind to lipids, including PA in plants.

ERD7 localizes in the vicinity of the cellular membrane

We next investigated the subcellular localization of ERD7 by isolating subcellular fractions from tissues taken from Arabidopsis plants exposed to 4°C LPA for 24 h. The identity of

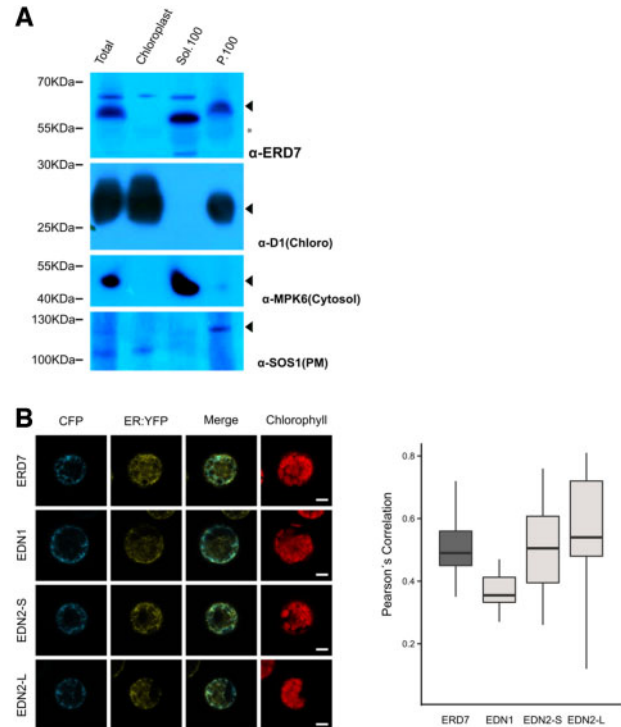


Fig. 3 ERD7 localization based on subcellular fractionation studies and confocal microscopy. (A) Cell extracts from plants treated with cold for 24 h were fractionated into the chloroplast, soluble (Sol.100) and microsomal fractions (P.100) and examined with anti-ERD7 antibody (arrowhead). The asterisk indicates background. Anti-D1, anti-MPK6 and anti-SOS1 antibodies were used as markers for chloroplast, cytosol and microsomal fractions, respectively, and are indicated by arrowheads. Twenty micrograms of total protein was loaded per lane. (B) Confocal microscopy analysis using mesophyll protoplasts from plants expressing YFP fused to the ER retention signal. The ERD7 family protein was fused to CFP. Co-localization between CFP and YFP is calculated based on Pearson's correlation showed by Coloc2 Plugin from Fiji. Bars: 10 μm. The figures are representatives for 10–11 biological replicates.

the fractions was validated with anti-D1, anti-MPK6 and anti-SOS1 antibodies as markers for the chloroplast, soluble and microsomal fractions, respectively. Anti-ERD7 recognized a ~58-kDa band only in the microsomal fraction (Fig. 3A). A band corresponding to a lower molecular weight was detected in the soluble fraction of both wild-type and *erd7* mutant plants, indicating that this was the background signal (Supplementary Fig. S3). To further examine the localization of the ERD7 family in cellular membranes, we constructed plasmids expressing ERD7 family proteins fused to a cyan fluorescent protein (CFP) to study its localization in mesophyll protoplast cells isolated from transgenic lines expressing ER markers fused to YFP protein (Nelson et al. 2007). Signals corresponding to ERD7, EDN1, EDN2 or EDN2-S did not overlap with the chlorophyll autofluorescence signal, indicating that the ERD7 family is not targeted to chloroplasts (Fig. 3B). On the other hand, the CFP signal did overlap with fluorescence signals arising from the ER-tagged YFP with a high degree of correlation. Note that not all signals were overlapped to the ER-YFP, suggesting that the ERD7 family is also localized at other

places, such as PM, and that the ERD7 family does not distribute uniformly to the whole ER membrane. These results supported that ERD7 localized in the vicinity of cellular membranes (Fig. 3B).

Mutant plants lacking the ERD7 family show developmental defects

To analyze the biological role of ERD7 *in vivo*, *erd7* mutant plants were isolated in Arabidopsis. The mutant lines showed no observable phenotype under several stress conditions, although Western blotting showed that the mutants lacked the ERD7 protein (Fig. 1). This result may be due to the presence of the two close ERD7 homologs EDN1 and EDN2. To produce higher-order mutants, we crossed the mutant lines (Fig. 4A) and genotyped the progeny by PCR. We identified semi-triple mutant *erd7^{+/-} edn2^{-/-} edn1^{-/-}* lines (heterozygous for ERD7 and homozygous for two close homologs: hereafter *hHH*). RT-PCR showed that there were no *EDN1* or *EDN2* mRNA in *hHH* (Supplementary Fig. S4A). In their progenies, no triple mutant was found and there were some empty spots in the silique of *hHH* (Supplementary Fig. S4B), suggesting that the triple mutant is embryonic lethal. In addition, the ratio of *hHH* was less (47%) than that expected based on the Mendelian rule (67%), suggesting that some *hHH* could not survive either. Since we could isolate three single mutants and two double mutants (*erd7^{-/-} edn2^{-/-}* and *edn2^{-/-} edn1^{-/-}*), the gene dosage of the ERD7 family may affect developmental success. *hHH* plants were found to have shorter petioles and rounded rosette leaves (Fig. 4B), while leaf mass per unit area was similar between *hHH* and wild-type plants (WT: 16.9 ± 2.9 , *hHH*: 16.0 ± 2.6 mg cm⁻², $n = 6$), and *hHH* plants fully developed and produced seeds. When ERD7 was expressed under 35S promoter, *hHH* plants had longer leaves compared to *hHH* plants without the exogenous expression (Supplementary Fig. S5A), although they were shorter than those of the wild type; this is probably because *EDN1* or *EDN2* were still lacking. Taken together, these results support an essential function for ERD7 family genes during plant development.

hHH mutants have diminished cold acclimation capacity

Due to the accumulation of ERD7 protein in response to low temperature, we next examined *hHH* cold tolerance. We transferred 6-week-old WT and *hHH* plants to a 4°C chamber for 10 d before evaluating anthocyanin accumulation as a sign of stress and ROS production (Xu et al. 2017). Both WT and *hHH* plants displayed higher anthocyanin content after 10 d at 4°C relative to plants maintained under normal growth conditions. However, *hHH* plants accumulated more anthocyanin than cold-treated WT plants (Fig. 5A) while the accumulation of anthocyanin was lower in the *hHH* plants transformed with 35S-ERD7 (Supplementary Fig. S5B).

We also evaluated the acclimation capacity of *hHH* plants by measuring the freezing tolerance of leaves taken from WT and *hHH* plants with or without pre-incubation at 4°C, by determining LT50 value (a parameter showing at which temperature 50% cell disruption occurs). WT plants had an LT50 of -4.8°C ,

whereas the LT50 for *hHH* was -3.4°C , indicating that *hHH* plants are slightly more sensitive to freezing temperatures than WT plants under basal condition. After an acclimation period, the WT LT50 was -9.9°C , but *hHH* had an LT50 of only -6.1°C (Fig. 5B), indicating that *hHH* plants also had considerably diminished cold acclimation capacity. The *hHH* plants transformed with 35S-ERD7 were more tolerant to freezing conditions after acclimation than *hHH* plants and the cold acclimation capacity was partly restored (Supplementary Fig. S5C).

Furthermore, we analyzed the cold-induced gene expression. RNA was extracted from rosette leaves before and after cold treatment (3 and 12 h at 4°C). Although an induction in all analyzed genes was detected in *hHH* plants, the induction of some genes, including COR15A, CBF3 and CBF2, was lower compared to that in the WT (Fig. 5C). These results indicate that cold-induced gene expression is also affected in the *hHH* plants.

hHH plants have a distinct membrane lipid composition

Based on the connection between the lipid composition of cellular membranes and cold acclimation in plants (Steponkus 1984, Degenkolbe et al. 2012), we carried out a comparative analysis of the lipid composition in *hHH* and WT plants. Total lipids were extracted from plants grown under normal growth conditions or at 4°C for 24 h and analyzed by mass spectrometry. The results showed that several lipid species were altered in *hHH* plants compared to wild type (Supplementary Table S1, Supplementary Fig. S6). To explore the correlation between the different lipids, and the different conditions and mutants, we performed a principal components analysis (PCA). The PCA showed separation between the four different experimental situations according to plant genotype and treatments (Fig. 6A, Supplementary Table S2). The distribution between control and cold-treated plants could be explained by increases in the level of several PC and PE species that had a high degree of saturation (e.g. PC(36:6), PE(36:5) and PE(36:4)). In addition, both *hHH* and WT plants had reduced levels of several MGDG species (mainly MGDG34:3, MGDG34:5, MGDG34:4 and MGDG 36:5) in response to cold, suggesting that they are relevant for the acclimation. These data are in agreement with previous comprehensive studies on lipid composition remodeling during cold acclimation, which showed an increase in PC and PE species together with a decrease in MGDG/DGDG species (Wang et al. 2006, Degenkolbe et al. 2012). On the other hand, our PCA data indicated that differences between WT and *hHH* samples were due to lower amounts of several MGDG/DGDG species, such as MGDG38:5, MGDG34:1, DGDG34:1 and DGDG36:4, in *hHH* cell membranes compared to those from WT, which were similar to those seen for non-acclimated plants (Fig. 6B). Together, these results indicated that the lipid composition of cellular membranes from *hHH* and WT plants differs and this difference could be related to the altered capacity to adapt to low temperatures, although they could not be directly correlated to previously reported mechanisms of cold acclimation.

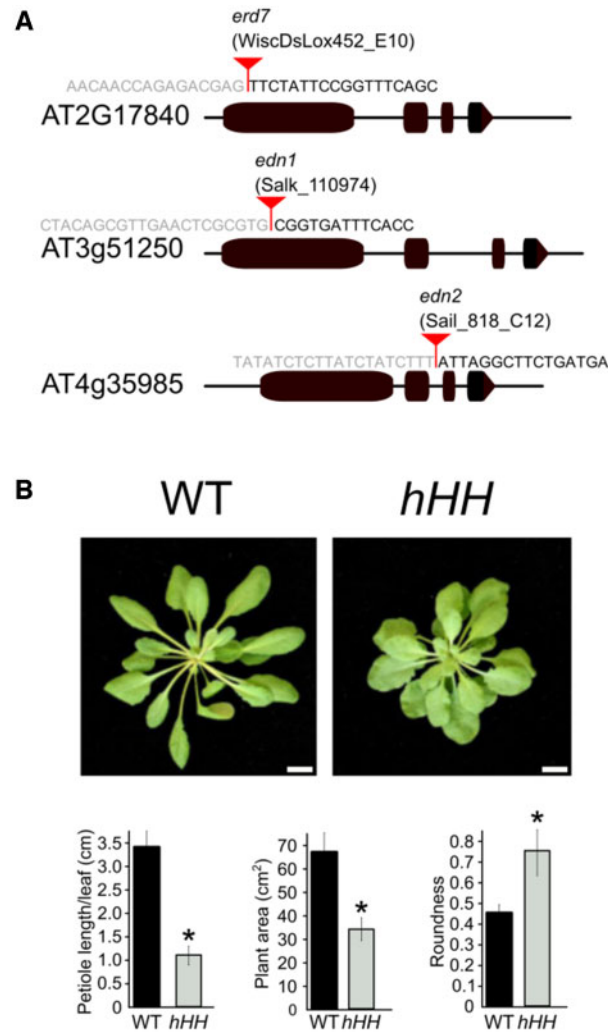


Fig. 4 Phenotypic comparison between WT and *hHH* plants. (A) Scheme of the three ERD7 gene family members and T-DNA insertion sites. (B) Morphological characterization of *hHH* plants. Pictures are of 6-week-old plants grown under SD conditions. Bars: 1 cm. Plant area, length of petiole per leaf and leaf roundness (plant area/total leaf area) were quantified (mean \pm SD, $n = 5$ biological replicates). $P < 0.05$ in Student's *t*-test.

ERD7 affects PPI metabolism

We used *in vivo* radiolabeling (Mishkind et al. 2009, Arisz et al. 2013) to determine whether defects in the ERD7 family affect the metabolism of PPIs or PA, as they have also been implicated in cold signaling (Ruelland et al. 2002, Delage et al. 2012, Arisz et al. 2013). The amount of PIP₂ was reduced by almost 50% in *hHH* plants compared to WT plants after exposure to cold for 30 min (Fig. 7). Overall PIP content was not significantly different while the response in PA was slightly less in *hHH* plants. These results indicate that ERD7 mediates not only the content of structural lipids but also the metabolism of PIP₂.

Since PIP₂ can be cleaved by PI-specific phospholipase C (PLC) to generate IP₃ and DAG, of which the latter can be phosphorylated to PA under cold conditions (Ruelland et al. 2002, Delage et al. 2012, Arisz et al. 2013), we measured the expression of PLC isoforms. Earlier work had shown that the expression of *PLC1*, -3, -4, -5 and -7 were upregulated upon cold treatment (Tasma et al. 2008). We found induced expression for *PLC3* and *PLC5* under our conditions but found no significant

difference between WT and *hHH* plants (Supplementary Fig. S7).

hHH mutants showed lesser membrane flexibility than WT

Cell membrane properties are related to lipid composition, mobility of lipids and molecular dynamics of the membrane due to protein binding to either of immobilized or fluid membrane domain. We used here Electron Paramagnetic Resonance (EPR) spin labeling to explore whether cell membranes in WT and *hHH* plants behave differently at diverse temperatures. In EPR, a spin label containing a spin sensitive reporter group (nitroxyl group) bound at a specific carbon position in the steric acid chain can be introduced into biological systems to detect changes in membrane composition and/or biophysical properties. In this case, it was used to detect changes in membrane fluidity. We incorporated a 16-doxy stearic acid (16DS) spin probe, which is used to study membrane fluidity in the interior of the hydrophobic core of the lipid bilayer in

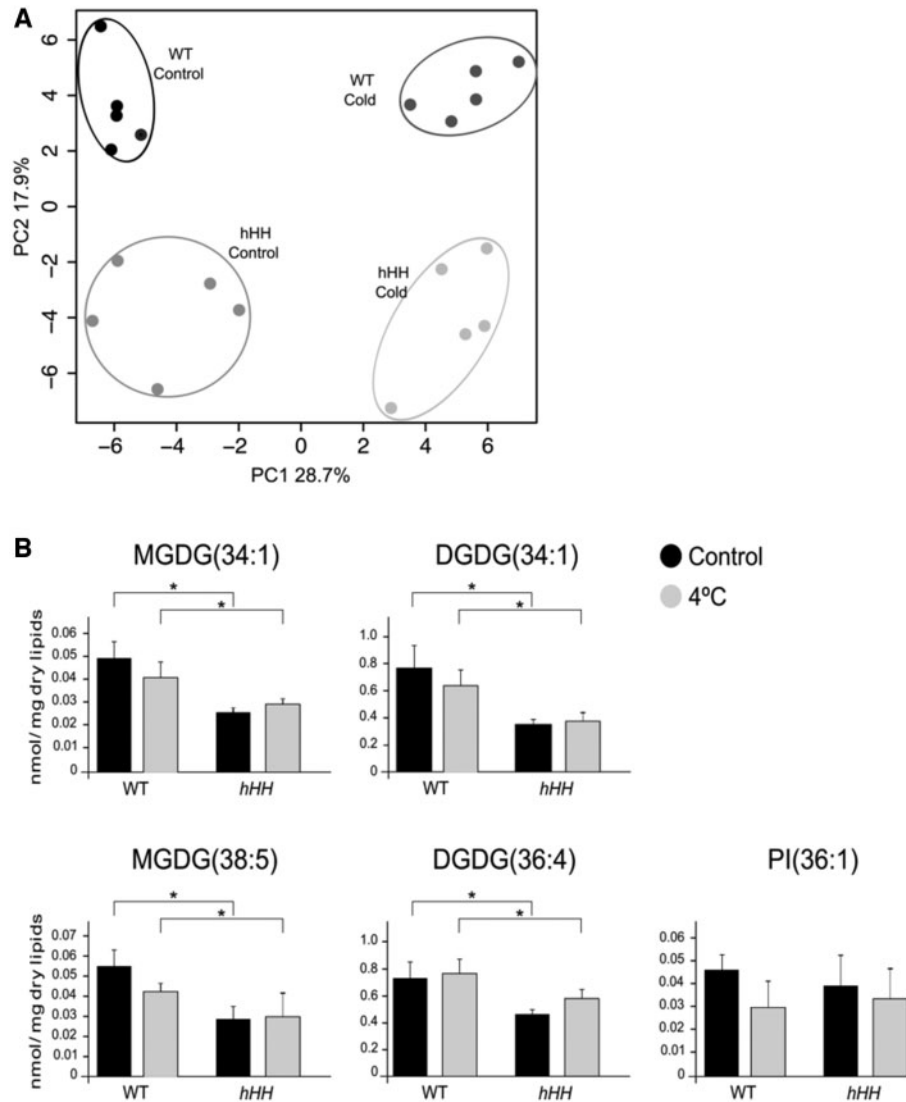


Fig. 6 Lipidome analysis. (A) Lipid content quantified by mass spectrometry. The PCA discerned between genotypes and between treatments to explain 46.6% of the total variance. (B) Amount of lipid species responsible for PCA distribution between genotypes (mean \pm SD, $n = 5$ biological replicates). * $P < 0.05$ in Student's t-test.

mutant with respect to WT, indicating that the ERD7 family in WT has lowered the activation energy for rotational diffusion. By contrast, no significant difference was observed in similar experiments using thylakoids (Supplementary Fig. S8). These results indicate that PMs of *hHH* plants are more rigid than WT membranes, and this effect is amplified at lower temperatures.

Discussion

ERD7 gene expression is induced in response to several abiotic stresses, such as drought, dehydration, cold, salt and light excess (Kiyosue et al. 1994, Taji et al. 1999, Kimura et al. 2003, Bray 2004, Sánchez et al. 2004, Kaplan et al. 2006). However, the function of ERD7 is unclear. In this study, we aimed to assign a functional role for ERD7 during plant stress. We showed

that ERD7 protein accumulates under various stress conditions, particularly following exposure to low temperature (Fig. 1). Attempts to generate a true triple mutant that lacked all three members of the ERD7 gene family were unsuccessful, likely due to embryo lethality. However, we did generate a semi-triple mutant, *hHH*, having the genotype *erd7^{+/-} edn2^{-/-} edn1^{-/-}*. Under normal growth conditions, *hHH* plants had a more compact morphology than WT (Fig. 4), indicating that ERD7 family genes are essential for normal growth and development.

In addition to growth and development, we have observed that ERD7 accumulates under several stress conditions (Fig. 1), suggesting a protective role in response to environmental stresses. Indeed, *hHH* plants were more susceptible to low temperatures and had reduced their cold acclimation capacity (Fig. 5). These data indicate that the ERD7 family promotes cold and freezing tolerance in plants.

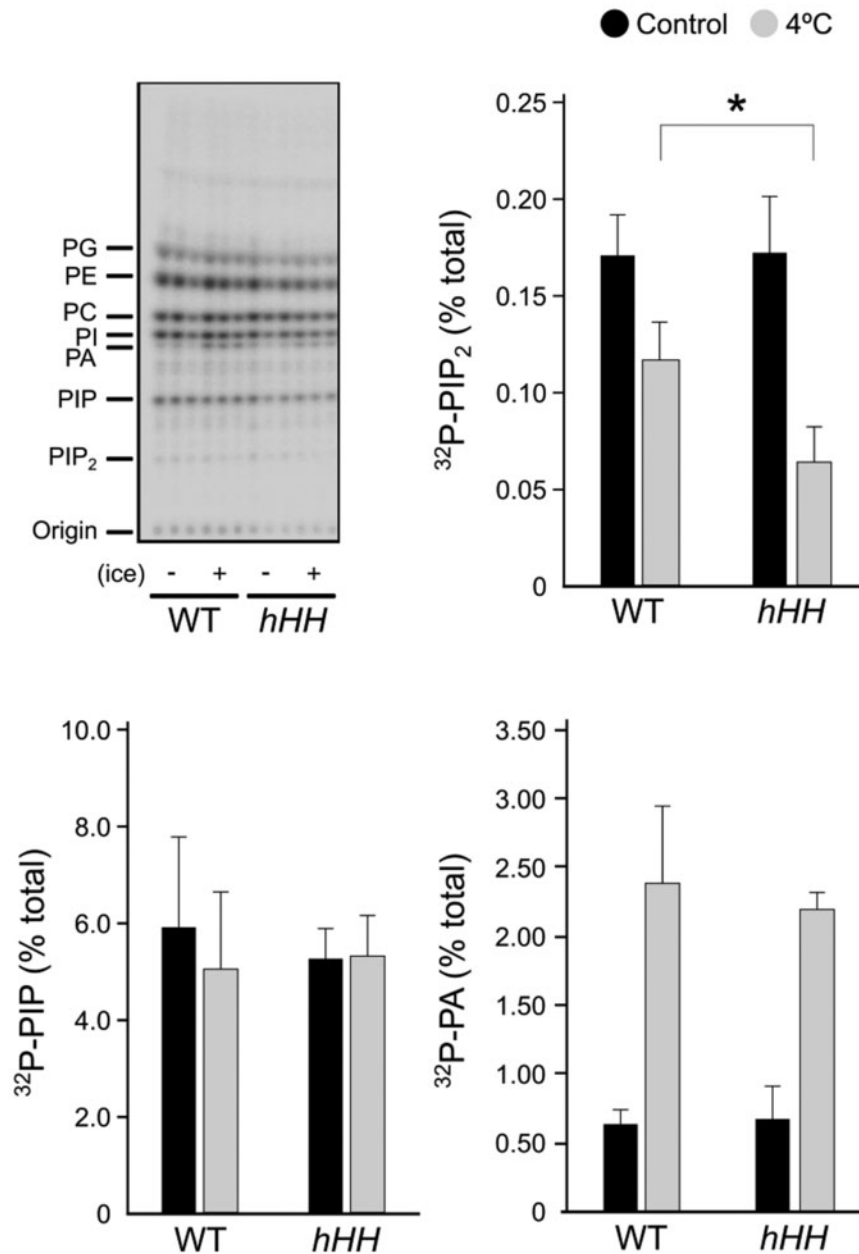


Fig. 7 PA and PPI measurements. Amounts of ^{32}P -labeled PIP_2 , PIP and PA were measured in WT and *hHH* plant leaf disks that were cold-stressed for 30 min. Phospholipids were separated by TLC (left) and quantified by PImaging (right). Results show the mean \pm SD ($n = 6$ biological replicates). $P < 0.05$ in Student's t -test.

Because ERD7 binds to negatively charged phospholipids, such as PI and PA (Fig. 2), we investigated the connection between ERD7 and lipids. Our protein–lipid assay could not discern specificity between ERD7 and any particular phospholipid species. The Senescence domain of ERD7 has a high pI value (9.79 according to ExPASy Compute pI tool, https://web.expasy.org/compute_pi/) reflecting its positive charge at physiological pH that might facilitate nonspecific electrostatic interactions with negatively charged phospholipids. This characteristic could also explain the localization of ERD7 to the membrane as well as a tight association with the cellular membranes (Fig. 3). The binding of ERD7 to phospholipids could induce structural and mechanical changes in the membrane that affect membrane fluidity. EPR results (Fig. 8)

showed that *hHH* plants have a more rigid PM that could render them vulnerable to mechanical stress and dehydration forces exerted by extracellular ice that forms at freezing temperatures (Steponkus 1984, Thomashow 1999). To obtain these data, we have developed a new protocol that allows the stabilization of mesophyll protoplasts during both EPR-probe incubation and EPR measurements. This approach could be of value for future studies that require analysis of plant cell PMs.

Another possible functional role for the ERD7 family is mediating membrane lipid composition through membrane metabolism and/or trafficking. Some types of changes in lipid composition counteract the loss of membranes' integrity and reduce the risk of cold or freezing injury (Uemura and Steponkus 1999, Moellering

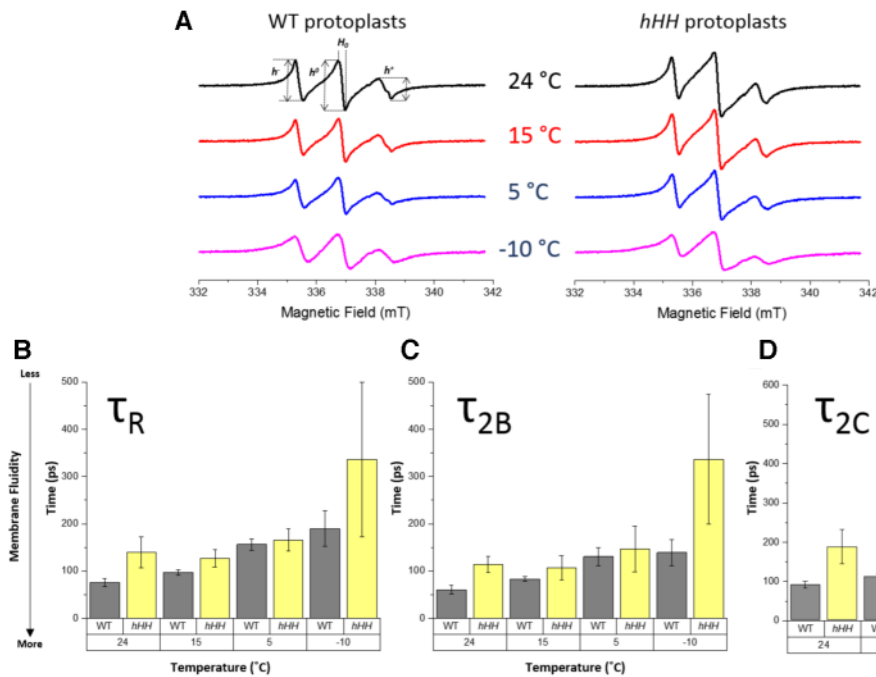


Fig. 8 EPR membrane fluidity measurements. (A) EPR spectrum of 16DS spin probe in protoplasts WT (left panel) and *hHH* mutant (right panel) measured at 24, 15, 5 and -10°C . Comparison of calculated values of (B) rotational correlation time (τ_R), (C) rotational correlation time along the axis (τ_{2B}) and (D) rotational correlation time perpendicular to the axis (τ_{2C}) from spectrum in (A). Each curve is an average of a minimum of three biological replicates. The EPR settings: center magnetic field, 336.95 mT; sweep width, ± 5 mT; modulation width, 0.1 mT; microwave power, 3 mW.

et al. 2010). Our lipidome analysis showed that general cold-induced effects occur in *hHH* plants (Fig. 6). Still, it cannot be excluded the possibility that differential accumulation of minor species affects the membrane feature via unknown mechanisms. Some MGDG species are reduced in *hHH* plants under normal conditions, which may cause higher sensitivity to freezing conditions without acclimation (Fig. 5B).

In addition, ERD7 may play a role in stress-responsive signaling. Some cold-induced gene expression was altered to some extent (Fig. 5C). The ERD7 family could affect cold-mediated signaling cascades that regulate the amount of PIP species. In particular, $\text{PI}(4,5)\text{P}_2$ is a source for DAG and IP_3 , which is a precursor of IP_6 , that act as signaling molecules and correlate with Ca^{2+} mobilization under stress conditions (DeWald et al. 2001, Krinke et al. 2006, Heilmann 2016). *hHH* plants showed a greater reduction in PIP_2 following exposure to cold (Fig. 7). Since no difference was detected in cold-induced levels of PLC expression between WT and *hHH* (Supplementary Fig. S7), the ERD7 family might mediate the PLC reaction through binding to PIPs. However, further studies are needed to determine the exact effect of ERD7 on PPI metabolism.

In summary, results in this study show that ERD7 interacts with phospholipids in cellular membranes. This interaction appears to affect lipid trafficking and/or metabolism and cellular membrane fluidity. Taken together, our findings indicated that the ERD7 gene family plays important role in both cold responses and development.

Materials and Methods

Plant material and phenotypic analyses

The *Arabidopsis thaliana* lines used in this study were Col-0 wild type, *erd7* (AT2G17840) (WISCDLSLOX452E10), AT3G51250 (Salk_110974) and AT4G35985 (Sail_818_C12). T-DNA insertion lines were obtained from the Arabidopsis Biological Resource Centre (Sessions et al., 2002, Alonso, 2003, Woody et al. 2007). Homozygous insertion lines were selected by PCR following the instructions (<http://signal.salk.edu/cgi-bin/tdnaexpress>). The following conditions were used: $1 \times 95^{\circ}\text{C}$ for 5 min; $35 \times (95^{\circ}\text{C}$ for 20 s, 55°C for 20 s, 70°C for 1 min) with primers described in Supplementary Table S3. The insertion sites were identified by sequencing of the amplicons. To generate the complementation line, ERD7 cDNA was cloned in pCAMBIA1300 with 35S promoter (pRT105) and transformed with *Agrobacterium* GV3100. Transformants were screened with hygromycin and PCR for genotyping.

Seeds were frozen for 24 h at -80°C to reduce the likelihood of insect contamination before transfer to soil and stratification at 4°C for 2 d in the dark. Mature plants were grown in soil for 6 weeks under short-day (SD) conditions ($120 \mu\text{mol photons m}^{-2} \text{s}^{-1}$, 8 h light/16 h darkness, 22°C).

For the evaluation of ERD7 protein content under different stress conditions, Col-0 and *erd7* seedlings grew in 1/2 Murashige and Skoog (MS) media plates supplemented with 1% sucrose under long-day conditions ($120 \mu\text{mol photons m}^{-2} \text{s}^{-1}$, 16 h light/8 h darkness, 22°C). After 10 d, some of the seedlings were transferred to Petri dishes containing 1/2 MS liquid media + 1% sucrose and 100 mM NaCl or 50 μM ABA for 1 h. For cold treatments, seedlings were incubated at 4°C for 24 h in Petri dishes with 1/2 MS media + 1% sucrose.

Anthocyanin levels were measured according to Loreti et al. (Loreti et al., 2008). For the measurement of leaf mass per area, similar-sized rosette leaves were compared between WT and the mutant. Plant area, length of petiole per leaf, leaf roundness (plant area/total leave area) and plant diameter were quantified using LeafJ plugin for FIJI software (Malooof et al. 2013).

ERD7 protein localization

To determine the subcellular localization of ERD7, full-length ERD7 and homolog cDNAs were amplified from Col-0 cDNA or cDNA in pGEX plasmids using the primer pairs in **Supplementary Table S3**. The amplicon was cloned into the binary plasmid pm-ck CD3-1001 (NASC) containing CFP following digestion with *XbaI/BamHI*. The resulting construct ERD7-CFP was transferred into mesophyll protoplasts isolated from different plants expressing different organelle markers as described in [Wu et al. \(2009\)](#). Fluorescence emission from YFP, CFP and chlorophyll was monitored using an SP2 confocal laser scanning system equipped with an inverted microscope. Confocal images were generated with Zeiss Zen 2012 software version 8.0.0.273 (<http://www.zeiss.com>). For the colocalization analysis, we made use of the Coloc2 plugin after the removal of images' background.

Western blotting

To detect ERD7 protein, an anti-ERD7 antibody was generated by immunizing rabbits with the synthetic peptide CRPTKEISHDSSDEEDGD that includes amino acids 141–157 of ERD7 as an antigen. The antibody was produced by AgriSera (product number: AS19 4317, 57, SE-911 21, Vännäs, Sweden).

Total protein was extracted from 5-week-old plants grown in the SD conditions. Tissue was collected and ground in liquid nitrogen. Protein extracts were generated using protein extraction buffer (Tris-HCl 50 mM, pH 8.0, 150 mM NaCl, 1% Triton X-100, 0.1% SDS, 0.5% Na-Deoxycholate, 2 mM phenylmethanesulfonyl fluoride, 2 mM dithiothreitol).

Isolation of microsomes and chloroplasts was performed according to [Abas and Luschig \(2010\)](#) and [Koskela et al. \(2018\)](#). Protein content was quantified using the Bradford method ([Bradford 1976](#)), and protein analysis was performed as described previously ([Barajas-Lopez et al. 2018](#)) using anti-ERD7, anti-MPK6 (AgriSera), anti-D1 (AgriSera) and anti-SOS1 ([Quintero et al. 2002](#)) antibodies.

Freezing damage measured by electrolyte leakage

WT and *hHH* plants were grown in the SD condition for 6 weeks. Fully developed leaves from cold-acclimated (4°C during 10 d) or non-acclimated plants were excised at the base of the petiole and placed in 15-ml Falcon tubes containing 1 ml of deionized water. The tubes were placed in a circulating water bath at 0°C and incubated for 30 min to allow temperature equilibration. The temperature was then decreased from 0 to –15°C at a rate of 2°C per hour. At the indicated temperatures, the tubes were removed from the water bath and immediately placed on ice to allow gradual thawing. The contents of each tube were transferred to new tubes containing 25 ml of deionized water, and the conductivity of the solution in each tube was measured. The percentage of electrolyte leakage was determined as the ratio of conductivity before autoclaving to that after autoclaving.

Impairment of detached leaves after a freeze–thaw cycle can be used to accurately quantify plant freezing tolerance in terms of LT50 values. LT50 values were calculated by fitting data into a sigmoidal model using environment v.3.1.1 ([R Development Core Team 2011](#)).

Lipid quantification

Full rosettes from 6-week-old plants grown in SD conditions were quickly immersed in glass tubes with Teflon-lined screw caps that contained 5 ml of isopropanol with 0.01% dibutylhydroxytoluene (BHT) and were incubated at 75°C for 15 min. Chloroform (1.5 ml) and water (0.6 ml) were added and incubated in a shaking incubator at room temperature for 1 h. Lipid extracts were then transferred to a new glass tube where 4 ml of chloroform:methanol (2:1) mixture with 0.01% BHT was added. The tube was shaken for 30 min, and we repeated this extraction procedure on all samples until the leaves were white. All the extractions were collected and 1 ml of KCl (1 M) solution was added to the combined extract. The mixture was vortexed and centrifuged to separate the phases. Finally, the lipid phase was washed with 2 ml of water before drying. Dried lipids were weighed and diluted in hexane to equal lipid concentrations. Lipidomics analyses were performed by the Kansas Lipidomics Research Center (<http://www.k-state.edu/lipid/lipidomics>). Raw data were normalized following a sample-centric approach and log₁₀-transformed. Centered and scaled values (z-scores) were subjected to PCA. PCA was performed in the R

environment v.3.1.1 ([R Development Core Team 2011](#)) using mixOmics v.4.0.2 ([Rohart et al. 2017](#)).

Lipid-binding assay

A truncated peptide from ERD7 (aas 69–440) that contained the Senescence domain (aas 258–427) was fused to the C-terminus of the MBP epitope. The recombinant protein was purified with amylose resin and used in a Lipid-Binding Assay with Membrane Lipid strip (Echelon Bioscience, 75 Arapeen Dr Ste 302, Salt Lake City, Utah 84108 US) as described previously ([Joshi and Bakowska 2011](#)). Liposome flotation assay was performed according to [Tronchere and Boal \(2017\)](#) with PC (Sigma-Aldrich, Feldbergstrasse 80, Darmstadt, 64293, Germany) and PA (Sigma-Aldrich). Centrifuged sucrose gradient (500 μl) was separated into five fractions (100 μl each), followed by Western blotting with anti-GST antibody (Upstate, 3 Trask Lane, Danvers, MA, 01923, US). To produce GST-fused recombinant proteins, cDNAs were amplified by PCR with primers (**Supplementary Table S3**) and cloned into pGEX-4T1. The proteins were purified as described previously ([Barajas-Lopez et al. 2018](#)). For the overlay assay with plant extract, 10 μg of lipids extracted as described above or PC from egg yolk (Sigma-Aldrich) were resolved in chloroform and blotted onto methanol-activated polyvinylidene fluoride membrane. After dried and soaked in methanol, the membrane was blocked with fat-free bovine serum albumin (BSA, Sigma-Aldrich) for the binding assay.

³²P_i-phospholipid labeling, extraction and analysis

Phospholipid levels were measured as described earlier ([Munnik and Zarza 2013](#)). Briefly, leaf disks (∅ 5 mm) were excised from 4-week-old Arabidopsis plants grown at SD conditions (11/13 h light/dark). Leaf disks were metabolically labeled overnight by flotation on 200 μl of incubation buffer (2.5 mM MES-KOH, pH 5.7, 1 mM KCl) containing 2.5–10 μCi ³²P_i (³²P_i; carrier free, 2.5–10 μCi μl⁻¹) in 2-ml safe-lock Eppendorf tubes in continuous light. Treatments were performed by placing tubes on ice water and stopped after 30 min by adding perchloric acid ([Munnik and Zarza 2013](#)). Lipids were extracted and analyzed by thin-layer chromatography (TLC) using alkaline and ethyl acetate solvent systems ([Munnik and Laxalt 2013](#), [Munnik and Zarza 2013](#)). Radioactivity was visualized by autoradiography, and individual lipids were quantified by phosphoimaging (Typhoon FLA 7000; GE Healthcare, 3350 North Ridge Avenue Arlington Heights, IL 60004 US).

EPR analysis

To assess cell membrane fluidity, chloroplast was isolated following a similar protocol described by [Koskela et al. \(2018\)](#). Briefly, fresh Arabidopsis leaves were gently blended in grinding buffer (330 mM sorbitol, 50 mM HEPES-KOH, pH 7.6, 1 mM MgCl₂ and 5 mM Na-EDTA, 0.1% BSA, 5 mM ascorbate). The suspension was filtered through two layers of Miracloth that had been presoaked with the grinding buffer. Filtrates were then centrifuged at 1,000 × g for 5 min and the resulting pellets were carefully resuspended in a small volume of grinding buffer. The resuspended pellet in grinding buffer was gently loaded on the top of 40:70% percoll gradient and subsequently tubes were centrifuged at 4,000 × g for 10 min. The intact chloroplasts were collected from the interphase and washed twice with washing buffer (330 mM sorbitol, 50 mM HEPES-KOH, pH 7.6, 2 mM Na-EDTA). The number of chloroplasts was quantified based on the chlorophyll content measured by spectrophotometry ([Porra et al. 1989](#)). Chloroplast thylakoids were obtained after resuspension of the chloroplasts in shock buffer (50 mM HEPES-KOH, pH 7.6, 5 mM sorbitol, 5 mM MgCl₂) and two freeze–thaw cycles. Mesophyll protoplast cells were isolated as described above except that the cells were stabilized in stab-buffer (154 mM NaCl, 125 mM, CaCl₂, 5 mM KCl, 5 mM glucose, 2 mM MES, pH 5.7, and 400 mM mannitol).

Membrane fluidity measurements were performed in protoplasts from wild-type and *hHH* mutant Arabidopsis plants using a spin-label 16DS with doxyl moiety present at the 16th carbonyl group in the stearic acid chain. The spin trap in chloroform (2.5 μl) was first added to the bottom of the tube and chloroform was evaporated. Subsequently, 50 μl of protoplast suspension equivalent to 25 μg chlorophyll was added to make 5 mM of the final concentration of spin trap in protoplasts. The labeling of protoplast with spin trap was performed by gently shaking the protoplast suspension on the spin trap for 30 min before the measurements. The measurements using 16DS were

performed at 22, 15, 5 and -10°C on Miniscope (MS5000) EPR spectrometer using a variable temperature accessory (TC-HO4) in a $50\text{-}\mu\text{l}$ capillary. The EPR settings used were a center magnetic field of 336.95 mT with a sweep width of $\pm 5\text{ mT}$, a modulation width of 0.1 mT and a microwave power of 3 mW . The final concentration of spin-label used in chloroplasts was $150\text{ }\mu\text{M}$ 16DS for each $50\text{ }\mu\text{g}$ of chlorophyll.

The rotational motion of the nitroxyl group inside the membrane was calculated as rotational correlation time (τ_R) from EPR spectra using the formula explained earlier (Ježek and Freisleben 1994). Any disorder in spin probe's motion either in parallel or perpendicular to membrane plane generates an anisotropy of the EPR spectrum, which are manifested in the calculated values of rotational correlation time along the axis (τ_{2B}) and perpendicular to the axis (τ_{2C}), respectively. The values of τ_{2B} and τ_{2C} were calculated as explained previously (Strzalka et al. 1995).

quantitative PCR (qPCR)

qPCR was performed following Tasma et al. (2008) using TIP41like (AT4g32370) as a reference gene. Primers that are not described in Tasma et al. (2008) are shown in Supplementary Table S3.

Supplementary Data

Supplementary data are available at PCP online.

Funding

The Turku Collegium for Science and Medicine and the Academy of Finland (Projects numbers 259169, 263853, 271832, 292763, 307335) to H.F. and Academy of Finland post-doctoral grant (Projects number 325122) to J.P.

Acknowledgments

The authors thank the Arabidopsis Biological Resource Center for providing the T-DNA insertion mutants. The authors acknowledge Prof. Eva-Mari Aro and Dr. Sajjaliisa Kangasjärvi for sharing antibodies and helpful discussion.

Disclosures

The authors declare that there is no conflict of interest.

References

- Abas, L. and Luschnig, C. (2010) Maximum yields of microsomal-type membranes from small amounts of plant material without requiring ultracentrifugation. *Anal. Biochem.* 401: 217–227.
- Alonso, J. M. (2003) Genome-Wide Insertional Mutagenesis of Arabidopsis thaliana. *Science* 301: 653–657.10.1126/science.1086391
- Arisz, S.A., Heo, J.-Y., Koevoets, I.T., Zhao, T., van Egmond, P., Meyer, J., et al. (2018) Diacylglycerol acyltransferase 1 contributes to freezing tolerance. *Plant Physiol.* 177: 1410–1424.
- Arisz, S.A., van Wijk, R., Roels, W., Zhu, J.-K., Haring, M.A. and Munnik, T. (2013) Rapid phosphatidic acid accumulation in response to low temperature stress in Arabidopsis is generated through diacylglycerol kinase. *Front. Plant Sci.* 4: 1–15.
- Barajas-Lopez, J.D., Moreno, J.R., Gamez-Arjona, F.M., Pardo, J.M., Punkkinen, M., Zhu, J.-K.K., et al. (2018) Upstream kinases of plant SnRKs are involved in salt stress tolerance. *Plant J.* 93: 107–118.
- Bradford, M.M. (1976) A rapid and sensitive method for the quantitation of microgram quantities of protein utilizing the principle of protein-dye binding. *Anal. Biochem.* 72: 248–254.
- Bray, E.A. (2004) Genes commonly regulated by water-deficit stress in *Arabidopsis thaliana*. *J. Exp. Bot.* 55: 2331–2341.
- Daboussi, L., Costaguta, G. and Payne, G.S. (2012) Phosphoinositide-mediated clathrin adaptor progression at the trans-Golgi network. *Nat. Cell Biol.* 14: 239–248.
- Degenkolbe, T., Giavalisco, P., Zuther, E., Seiwert, B., Hincha, D.K. and Willmitzer, L. (2012) Differential remodeling of the lipidome during cold acclimation in natural accessions of *Arabidopsis thaliana*. *Plant J.* 72: 972–982.
- Delage, E., Ruelland, E., Guillas, I., Zachowski, A. and Puyaubert, J. (2012) Arabidopsis type-III phosphatidylinositol 4-kinases $\beta 1$ and $\beta 2$ are upstream of the phospholipase C pathway triggered by cold exposure. *Plant Cell Physiol.* 53: 565–576.
- DeWald, D.B., Torabinejad, J., Jones, C.A., Shope, J.C., Cangelosi, A.R., Thompson, J.E., et al. (2001) Rapid accumulation of phosphatidylinositol 4,5-bisphosphate and inositol 1,4,5-trisphosphate correlates with calcium mobilization in salt-stressed Arabidopsis. *Plant Physiol.* 126: 759–769.
- Eriksson, S.K., Kutzer, M., Procek, J., Gröbner, G. and Harryson, P. (2011) Tunable membrane binding of the intrinsically disordered dehydrin Lti30, a cold-induced plant stress protein. *Plant Cell* 23: 2391–2404.
- Hammond, J.P., Bennett, M.J., Bowen, H.C., Broadley, M.R., Eastwood, D.C., May, S.T., et al. (2003) Changes in gene expression in Arabidopsis shoots during phosphate starvation and the potential for developing smart plants. *Plant Physiol.* 132: 578–596.
- Heilmann, I. (2016) Phosphoinositide signaling in plant development. *Development* 143: 2044–2055.
- Hou, Q., Ufer, G. and Bartels, D. (2016) Lipid signalling in plant responses to abiotic stress. *Plant Cell Environ.* 39: 1029–1048.
- Hruz, T., Laule, O., Szabo, G., Wessendorp, F., Bleuler, S., Oertle, L., et al. (2008) Genevestigator V3: A reference expression database for the meta-analysis of transcriptomes. *Adv. Bioinformatics* 2008: 1–5.
- Ježek, P. and Freisleben, H.J. (1994) Fatty acid binding site of the mitochondrial uncoupling protein. Demonstration of its existence by EPR spectroscopy of 5-DOXYL-stearic acid. *FEBS Lett.* 343: 22–26.
- Joshi, D.C. and Bakowska, J.C. (2011) Spg20 protein spartin associates with cardiolipin via its plant-related senescence domain and regulates mitochondrial Ca^{2+} homeostasis. *PLoS One* 6: e19290.
- Kaplan, B., Davydov, O., Knight, H., Galon, Y., Knight, M.R., Fluhr, R., et al. (2006) Rapid transcriptome changes induced by cytosolic Ca^{2+} transients reveal ABRE-related sequences as Ca^{2+} -responsive cis elements in Arabidopsis. *Plant Cell* 18: 2733–2748.
- Kimura, M., Yamamoto, Y.Y., Seki, M., Sakurai, T., Sato, M., Abe, T., et al. (2003) Identification of Arabidopsis genes regulated by high light-stress using cDNA microarray. *Photochem. Photobiol.* 77: 226–233.
- Kiyosue, T., Yamaguchi-Shinozaki, K. and Shinozaki, K. (1994) Cloning of cDNAs for genes that are early-responsive to dehydration stress (ERDs) in *Arabidopsis thaliana* L: identification of three ERDs as HSP cognate genes. *Plant Mol. Biol.* 25: 791–798.
- Koskela, M.M., Brünje, A., Ivanauskaitė, A., Grabsztunowicz, M., Lassowskat, I., Neumann, U., et al. (2018) Chloroplast acetyltransferase NSI is required for state transitions in *Arabidopsis thaliana*. *Plant Cell* 30: 1695–1709.
- Kreps, J.A.A., Wu, Y., Chang, H.S., Zhu, T., Wang, X. and Harper, J.F. (2002) Transcriptome changes for Arabidopsis in response to salt, osmotic, and cold stress. *Plant Physiol.* 130: 2129–2141.
- Krinke, O., Novotná, Z., Valentová, O. and Martinec, J. (2006) Inositol triphosphate receptor in higher plants: is it real? *J. Exp. Bot.* 58: 361–376.
- Liu, Y., Dang, P., Liu, L. and He, C. (2019) Cold acclimation by the CBF–COR pathway in a changing climate: lessons from *Arabidopsis thaliana*. *Plant Cell Rep.* 38: 511–519.

- Loreti, E., Povero, G., Novi, G., Solfanelli, C., Alpi, A. and Perata, P. (2008) Gibberellins, jasmonate and abscisic acid modulate the sucrose-induced expression of anthocyanin biosynthetic genes in Arabidopsis. *New Phytologist* 179: 1004
- Maloof, J.N., Nozue, K., Mumbach, M.R. and Palmer, C.M. (2013) Leafj: an imageJ plugin for semi-automated leaf shape measurement. *J. Vis. Exp.* 71: 50028.
- McLoughlin, F., Galvan-Ampudia, C.S., Julkowska, M.M., Caarls, L., Van Der Does, D., Laurière, C., et al. (2012) The Snf1-related protein kinases SnRK2.4 and SnRK2.10 are involved in maintenance of root system architecture during salt stress. *Plant J.* 72: 436–449.
- Mishkind, M., Vermeer, J.E.M., Darwish, E. and Munnik, T. (2009) Heat stress activates phospholipase D and triggers PIP2 accumulation at the plasma membrane and nucleus. *Plant J.* 60: 10–21.
- Moellering, E.R., Muthan, B. and Benning, C. (2010) Freezing tolerance in plants requires lipid remodeling at the outer chloroplast membrane. *Science* 330: 226–228.
- Munnik, T. and Lxalt, A.M. (2013) Measuring PLD activity in vivo. *Methods Mol. Biol.* 1009: 219–231.
- Munnik, T. and Nielsen, E. (2011) Green light for polyphosphoinositide signals in plants. *Curr. Opin. Plant Biol.* 14: 489–497.
- Munnik, T. and Vermeer, J.E.M. (2010) Osmotic stress-induced phosphoinositide and inositol phosphate signalling in plants. *Plant Cell Environ.* 33: 655–669.
- Munnik, T. and Zarza, X. (2013) Analyzing plant signaling phospholipids through ³²Pi-labeling and TLC. *Methods Mol. Biol.* 1009: 3–15.
- Navarro-Retamal, C., Bremer, A., Ingólfsson, H.I., Alzate-Morales, J., Caballero, J., Thalhammer, A., et al. (2018) Folding and lipid composition determine membrane interaction of the disordered protein COR15A. *Biophys. J.* 115: 968–980.
- Nelson, B.K., Cai, X. and Nebenführ, A. (2007) A multicolored set of in vivo organelle markers for co-localization studies in Arabidopsis and other plants. *Plant J.* 51: 1126–1136.
- Noack, L.C. and Jaillais, Y. (2017) Precision targeting by phosphoinositides: how PIs direct endomembrane trafficking in plants. *Curr. Opin. Plant Biol.* 40: 22–33.
- Petersen, J., Eriksson, S.K., Harryson, P., Pierog, S., Colby, T., Bartels, D., et al. (2012) The lysine-rich motif of intrinsically disordered stress protein CDeT11-24 from *Craterostigma plantagineum* is responsible for phosphatidic acid binding and protection of enzymes from damaging effects caused by desiccation. *J. Exp. Bot.* 63: 4919–4929.
- Porra, R.J., Thompson, W.A. and Kriedemann, P.E. (1989) Determination of accurate extinction coefficients and simultaneous equations for assaying chlorophylls a and b extracted with four different solvents: verification of the concentration of chlorophyll standards by atomic absorption spectroscopy. *BBA Bioenerg.* 975: 384–394.
- Quintero, F.J., Ohta, M., Shi, H., Zhu, J.-K. and Pardo, J.M. (2002) Reconstitution in yeast of the Arabidopsis SOS signaling pathway for Na⁺ homeostasis. *Proc. Natl. Acad. Sci. USA* 99: 9061–9066.
- R Development Core Team (2011) R: a language and environment for statistical computing. *R Found. Stat. Comput.* 3: 201.
- Rohart, F., Gautier, B., Singh, A. and Lê Cao, K.A. (2017) mixOmics: an R package for 'omics feature selection and multiple data integration. *PLoS Comput. Biol.* 13: e1005752.
- Roy Choudhury, S. and Pandey, S. (2017) Phosphatidic acid binding inhibits RGS1 activity to affect specific signaling pathways in Arabidopsis. *Plant J.* 90: 466–477.
- Ruelland, E., Cantrel, C., Gawer, M., Kader, J.C. and Zachowski, A. (2002) Activation of phospholipases C and D is an early response to a cold exposure in Arabidopsis suspension cells. *Plant Physiol.* 130: 999–1007.
- Sánchez, J.P., Duque, P. and Chua, N.H. (2004) ABA activates ADPR cyclase and cADPR induces a subset of ABA-responsive genes in Arabidopsis. *Plant J.* 38: 381–395.
- Sessions, A., Burke, E., Presting, G., Aux, G., Mcelver, J., Patton, D., et al. (2002) A High-Throughput Arabidopsis Reverse Genetics System. *Plant Cell* 14: 2985–2994.10.1105/tpc.004630
- Steponkus, P.L. (1984) Role of the plasma membrane in freezing injury and cold acclimation. *Annu. Rev. Plant Physiol.* 35: 543–584.
- Steponkus, P.L., Uemura, M., Joseph, R. A., Gilmour, S.J. and Thomashow, M. F. (1998) Mode of action of the COR15A gene on the freezing tolerance of *Arabidopsis thaliana*. *Proc. Natl. Acad. Sci. USA* 95: 14570–14575.
- Strzałka, K., Hara-Nishimura, I. and Nishimura, M. (1995) Changes in physical properties of vacuolar membrane during transformation of protein bodies into vacuoles in germinating pumpkin seeds. *BBA Biomembr.* 1239: 103–110.
- Taji, T., Seki, M., Yamaguchi-Shinozaki, K., Kamada, H., Giraudat, J. and Shinozaki, K. (1999) Mapping of 25 drought-inducible genes, RD and ERD, in *Arabidopsis thaliana*. *Plant Cell Physiol.* 40: 119–123.
- Tan, W.-J., Yang, Y.-C., Zhou, Y., Huang, L.-P., Xu, L., Chen, Q.-F., et al. (2018) DIACYLGLYCEROL ACYLTRANSFERASE and DIACYLGLYCEROL KINASE modulate triacylglycerol and phosphatidic acid production in the plant response to freezing stress. *Plant Physiol.* 177: 1303–1318.
- Tasma, I.M., Brendel, V., Whitham, S.A. and Bhattacharyya, M.K. (2008) Expression and evolution of the phosphoinositide-specific phospholipase C gene family in *Arabidopsis thaliana*. *Plant Physiol. Biochem.* 46: 627–637.
- Testerink, C. and Munnik, T. (2011) Molecular, cellular, and physiological responses to phosphatidic acid formation in plants. *J. Exp. Bot.* 62: 2349–2361.
- Thomashow, M.F. (1999) PLANT COLD ACCLIMATION: freezing tolerance genes and regulatory mechanisms. *Annu. Rev. Plant Physiol. Plant Mol. Biol.* 50: 571–599.
- Tronchere, H. and Boal, F. (2017) Liposome flotation assays for phosphoinositide-protein interaction. *Bio Protocol* 7: e2169
- Uemura, M., Joseph, R.A. and Steponkus, P.L. (1995) Cold acclimation of *Arabidopsis thaliana* (effect on plasma membrane lipid composition and freeze-induced lesions). *Plant Physiol.* 109: 15–30.
- Uemura, M. and Steponkus, P.L. (1999) Cold acclimation in plants: relationship between the lipid composition and the cryostability of the plasma membrane. *J. Plant Res.* 112: 245–254.
- Vermeer, J.E.M. and Munnik, T. (2013) Using genetically encoded fluorescent reporters to image lipid signalling in living plants. *Methods Mol. Biol.* 1009: 283–289.
- Wang, X.M., Li, W.Q., Li, M.Y. and Welti, R. (2006) Profiling lipid changes in plant response to low temperatures. *Physiol. Plant.* 126: 90–96.
- Webb, M.S., Uemura, M. and Steponkus, P.L. (1994) A comparison of freezing injury in oat and rye: two cereals at the extremes of freezing tolerance. *Plant Physiol.* 104: 467–478.
- Wu, F.H., Shen, S.C., Lee, L.Y., Lee, S.H., Chan, M.T. and Lin, C.S. (2009) Tape-Arabidopsis sandwich—a simpler Arabidopsis protoplast isolation method. *Plant Methods* 5: 16.
- Xu, Z., Mahmood, K. and Rothstein, S.J. (2017) ROS induces anthocyanin production via late biosynthetic genes and anthocyanin deficiency confers the hypersensitivity to ROS-generating stresses in Arabidopsis. *Plant Cell Physiol.* 58: 1364–1377.
- Yao, H.Y. and Xue, H.W. (2018) Phosphatidic acid plays key roles regulating plant development and stress responses. *J. Integr. Plant Biol.* 60: 851–863. (November 5, 2020, date last accessed).
- Yu, L., Nie, J., Cao, C., Jin, Y., Yan, M., Wang, F., et al. (2010) Phosphatidic acid mediates salt stress response by regulation of MPK6 in *Arabidopsis thaliana*. *New Phytol* 188: 762–773.
- Zhang, W., Qin, C., Zhao, J. and Wang, X. (2004) Phospholipase D α 1-derived phosphatidic acid interacts with ABI1 phosphatase 2C and regulates abscisic acid signaling. *Proc. Natl. Acad. Sci. USA* 101: 9508–9513.
- Zheng, G., Tian, B., Zhang, F., Tao, F. and Li, W. (2011) Plant adaptation to frequent alterations between high and low temperatures: remodelling of membrane lipids and maintenance of unsaturation levels. *Plant Cell Environ.* 34: 1431–1442.